Transepithelial resistance can be regulated by the intestinal brush-border Na+/H+ exchanger NHE3

Jerrold R. Turner, Eric D. Black, Jeff Ward, Chung-Ming Tse, Frederick A. Uchwat, Halima A. Alli, Mark Donowitz, James L. Madara and Jason M. Angle

Am J Physiol Cell Physiol 279:1918-1924, 2000.

Am J Physiol Cell Physiol
279: C1918–C1924, 2000.

Transepithelial resistance can be regulated by the intestinal brush-border Na^+/H^+ exchanger NHE3

JERROLD R. TURNER,[1] ERIC D. BLACK,[1] JEFF WARD,[2] CHUNG-MING TSE,[2]
FREDERICK A. UCHWAT,[1] HALIMA A. ALLI,[1] MARK DONOWITZ,[2]
JAMES L. MADARA,[3] AND JASON M. ANGLE[1]
[1]*Department of Pathology, Wayne State University School of Medicine, Detroit, Michigan 48201;*
[2]*Gastrointestinal Division, Department of Medicine, Johns Hopkins University School of Medicine, Baltimore, Maryland 21205; and* [3]*Department of Pathology, Emory University School of Medicine, Atlanta, Georgia 30322*

Received 23 March 2000; accepted in final form 4 August 2000

Turner, Jerrold R., Eric D. Black, Jeff Ward, Chung-Ming Tse, Frederick A. Uchwat, Halima A. Alli, Mark Donowitz, James L. Madara, and Jason M. Angle. Transepithelial resistance can be regulated by the intestinal brush-border Na^+/H^+ exchanger NHE3. *Am J Physiol Cell Physiol* 279: C1918–C1924, 2000.—Initiation of intestinal Na^+-glucose cotransport results in transient cell swelling and sustained increases in tight junction permeability. Since Na^+/H^+ exchange has been implicated in volume regulation after physiological cell swelling, we hypothesized that Na^+/H^+ exchange might also be required for Na^+-glucose cotransport-dependent tight junction regulation. In Caco-2 monolayers with active Na^+-glucose cotransport, inhibition of Na^+/H^+ exchange with 200 μM 5-(*N*,*N*-dimethyl)-amiloride induced 36 ± 2% increases in transepithelial resistance (TER). Evaluation using multiple Na^+/H^+ exchange inhibitors showed that inhibition of the Na^+/H^+ exchanger 3 (NHE3) isoform was most closely related to TER increases. TER increases due to NHE3 inhibition were related to cytoplasmic acidification because cytoplasmic alkalinization with 5 mM NH_4Cl prevented both cytoplasmic acidification and TER increases. However, NHE3 inhibition did not affect TER when Na^+-glucose cotransport was inhibited. Myosin II regulatory light chain (MLC) phosphorylation decreased up to 43 ± 5% after inhibition of Na^+/H^+ exchange, similar to previous studies that associate decreased MLC phosphorylation with increased TER after inhibition of Na^+-glucose cotransport. However, NHE3 inhibitors did not diminish Na^+-glucose cotransport. These data demonstrate that inhibition of NHE3 results in decreased MLC phosphorylation and increased TER and suggest that NHE3 may participate in the signaling pathway of Na^+-glucose cotransport-dependent tight junction regulation.

Na^+/H^+ exchange; tight junction regulation; Na^+-glucose cotransport

INTESTINAL EPITHELIAL CELLS integrate selective absorptive and secretory transport processes and also serve as barriers to passive transepithelial solute movement. Since hydrophilic and charged molecules are limited in their ability to traverse the lipid bilayer, the major pathway for passive transepithelial flux of such solutes is paracellular. The permeability of the paracellular pathway is primarily determined by the tight junction. Thus changes in tight junction permeability can regulate mucosal permeability to macromolecules.

We have described a cultured cell model that recapitulates physiological regulation of small intestinal villus enterocyte tight junctions by the activity of the apical intestinal Na^+-glucose cotransporter SGLT1 (22). As in native mucosa, initiation of Na^+-glucose cotransport in this model induces reversible 20–30% increases in tight junction permeability (1, 10, 22). Sodium glucose cotransport also leads to increases in phosphorylation of the myosin II regulatory light chain (MLC). This MLC phosphorylation can be prevented by pharmacological inhibition of MLC kinase (22), which also prevents increases in tight junction permeability (22). Thus MLC phosphorylation is a requisite intermediate in Na^+-glucose cotransport-dependent regulation of intestinal epithelial tight junctions (21, 22).

In addition to tight junction regulation, a well-recognized consequence of SGLT1-mediated Na^+-glucose cotransport is cell swelling. This triggers a regulatory volume decrease response that rapidly normalizes cell volume (8). Induction of similar degrees of cell swelling in isolated enterocytes by 5% hypotonic dilution also triggers regulatory volume decrease (9). In this case, regulatory volume decrease is prevented by inhibitors of Na^+/H^+ exchange (9). Since both tight junction regulation and regulatory volume decrease are consequences of apical Na^+-nutrient cotransport, we hypothesized that there may be overlap between the signaling pathways that regulate these events. Thus we explored the role of Na^+/H^+ exchange in Na^+-glucose cotransport-dependent tight junction regulation. The data show that inhibition of Na^+/H^+ exchange can increase transepithelial resistance (TER) and that the mechanisms by which this occurs may

Address for reprint requests and other correspondence: J. R. Turner, 540 E. Canfield, 9248 Scott Hall, Detroit, MI 48201 (E-mail: jturner@med.wayne.edu).

The costs of publication of this article were defrayed in part by the payment of page charges. The article must therefore be hereby marked "*advertisement*" in accordance with 18 U.S.C. Section 1734 solely to indicate this fact.

overlap with those involved in Na^+-glucose cotransport-dependent tight junction regulation.

METHODS

Materials. Tissue culture media and serum were from GIBCO (Life Technologies, Gaithersburg, MD). HOE-694 and S-3226 [an inhibitor of Na^+/H^+ exchanger 3 (NHE3)] were kind gifts from Dr. Hans-Jochen Lang, Hoechst-Marion Roussel, Germany (4, 15). All other Na^+/H^+ exchange inhibitors were from Sigma (St. Louis, MO). Monoclonal antibodies to MLC (clone MY-21) were from Sigma. Peroxidase-conjugated secondary antibodies for immunoblotting were from ICN (Costa Mesa, CA). ML-7 was from Calbiochem (La Jolla, CA).

Cell culture and preparation. Clonal populations of Caco-2 cells with active physiological Na^+-glucose cotransport were generated by stable transfection (20) and maintained in DMEM with 25 mM glucose (high-glucose DMEM) with 10% fetal calf serum, 15 mM HEPES, pH 7.4, and 0.25 mg/ml geneticin. For growth as monolayers, cells were plated on collagen-coated 0.4-μm pore size polycarbonate membrane Transwell supports (Corning-Costar, Cambridge, MA) and used 14–20 days postconfluence, as previously described (22). Transwell supports with 0.33- and 5-cm^2 surface area were used for electrophysiology and biochemical studies, respectively. For fluorometry, cells from a confluent flask were lightly trypsinized, replated onto collagen-coated coverslips, and used at 100% confluence after 4–5 days. Whether grown on Transwells or coverslips, cells were cultured in DMEM without geneticin before use in experiments. All experiments were performed in a physiological buffer [Hanks' balanced salt solution (HBSS)] with 25 mM glucose (to match that in the DMEM), 15 mM HEPES, and 4.2 mM $NaHCO_3$, except where noted. Except where noted, drugs were simultaneously added to both apical and basal compartments of Transwell supports.

Electrophysiology. Electrophysiological measurements were made using agar bridges and Ag-AgCl calomel electrodes. A 50-μA current was passed across the monolayers using a model 558 voltage clamp (Univ. of Iowa Bioengineering, Iowa City, IA). TER and short-circuit current were calculated using Ohm's law, as previously described (22).

Analysis of Na^+/H^+ exchanger isoform expression by RT-PCR. Confluent monolayers of Caco-2 cells grown on Transwell supports were lysed in TRIzol reagent (Life Technologies). Total RNA was annealed with oligo$(dT)_{12-18}$, and first-strand cDNA synthesis was carried out using SuperScript Preamplification System (GIBCO BRL). Primers for human NHE1 and NHE2 were designed from published sequences (GenBank accession nos. M81768 and AF073299, respectively; NHE1 sense, 5′-GTCTCCATGCAGAACATCCACC-3′, antisense, 5′-CAGTTCTGCCAAATGGATTGG-3′, nt 1863–2726; NHE2 sense, 5′-CATGCCATTGAGATGGCAGAGAC-3′, antisense, 5′-GCTTTCGCTGCTTCTCTTAAGG-3′, nt 1777–2545). Primers for human NHE3 (GenBank accession no. U28043) were published previously [sense (B13), 5′-CATGTGGACCTGGAACACG-3′, antisense (B14), 5′-CGTAGCTGATGGCATCCTTC-3′, nt 1086–1639] (3). Reactions (50 μl) were carried out in a PE/Applied Biosystems GeneAmp 9700 (Foster City, CA) for 30–35 cycles (45 s at 94°C, 45 s at 50°C, and 1.5 min at 72°C). PCR products (NHE1 and NHE3, 10 μl each, and NHE2, 50 μl) were analyzed on a 1.0% agarose gel. The authenticity of PCR products was confirmed by sequencing using PE/Applied Biosystems 377 Automated DNA Sequencer.

Sugar uptake assays. Sugar uptake assays were done in quadruplicate using cells grown on collagen-coated 1-cm^2 surface area tissue culture dishes (Corning-Costar). Briefly, wells were washed three times with glucose-free HBSS and then incubated for 20 min at 37°C with 0.4-ml glucose-free HBSS (with HEPES and $NaHCO_3$) that contained 100 μM [^{14}C]methyl α-glucoside (20) and the appropriate Na^+/H^+ exchange inhibitor. Wells were then washed four times with 4°C HBSS with 25 mM glucose, and cells were solubilized with 0.1 ml of 0.1 N NaOH. Specificity was confirmed by a 97% reduction in [^{14}C]methyl α-glucoside uptake when 1 mM phloridzin was added and a 92% decrease when 10 mM glucose was added. In contrast, 10 mM mannose, which is not transported by SGLT1, had no effect on [^{14}C]methyl α-glucoside uptake.

Analysis of MLC phosphorylation. Monolayers grown on 5-cm^2 Transwell supports were preloaded with 250 μCi/ml [^{32}P]orthophosphate (ICN, Costa Mesa, CA) as described previously (22). After incubation with Na^+/H^+ exchange inhibitors, incubations were terminated by washing the monolayers three times in 4°C PBS and scraping the cells into 200-μl of lysis buffer {25 mM Tris, pH 8.0, 100 mM sodium pyrophosphate, 100 mM NaF, 250 mM NaCl, 0.5% 3-[(3-cholamidopropyl)dimethylammonio]-1-propanesulfonate, 1% Triton X-100, 10 mM EGTA, 5 mM EDTA, 500 μM 4-(2-aminoethyl)benzenesulfonyl fluoride, 1 μM E-64, 1 μM leupeptin, and 1 μg/ml aprotinin}. Aliquots were then separated on 15% SDS-PAGE gels. ^{32}P incorporation into MLC was assessed by autoradiography and quantitative immunoblot, as described previously (22).

MLC phosphorylation was also determined using urea glycerol PAGE. For these analyses, monolayers were harvested by scraping cells into 4°C 10% trichloroacetic acid and 10 mM dithiothreitol. The pellets were washed three times with diethyl ether, dried, and solubilized in urea glycerol gel sample buffer (6.7 M urea, 10 mM dithiothreitol, 18 mM Tris, pH 8.6, 20 mM glycine, 5% saturated sucrose, and 0.004% bromphenol blue). Urea glycerol gels were performed as described (14, 17) using the Mini-PROTEAN II vertical electrophoresis system (Bio-Rad, Hercules, CA). Briefly, after preelectrophoresis at 300 V for 120 min at 25°C, samples were electrophoresed for 150 min at 300 V. After electrophoresis, the gels were equilibrated in 25 mM Na_2HPO_4, pH 7.6, transferred to polyvinylidene difluoride (Pall Gelman, Ann Arbor, MI) at 25°C for 90 min at 25 V, and immunoblotted for MLC as described previously (22).

Fluorometric measurement of intracellular pH. Confluent monolayers were washed twice with HBSS (with 25 mM glucose, 15 mM HEPES, and 4.2 mM $NaHCO_3$, except as noted) and then incubated for 15 min at room temperature with 3.5 μM 2′,7′-bis(2-carboxyethyl)-5(6)-carboxyfluorescein acetoxymethyl ester (BCECF-AM; Molecular Probes, Eugene, OR). After washing, BCECF-loaded cells were analyzed using a model RC-M fluorometer equipped with a dual-emission/excitation monochromator (Photon Technology International, Monmouth Junction, NJ). Fluorescence was measured at excitations of 439 and 502 nm and emission at 535 nm. Data were collected and analyzed using Felix software (version 1.21; Photon Technology International). For experiments in which HBSS without $NaHCO_3$ was used, this nominally HCO_3^--free buffer was also used for washing and BCECF loading.

Statistical analysis. All experiments were performed multiple times with duplicate or triplicate samples in each experiment. Results are expressed as means ± SE. Conditions were compared using Student's *t*-test.

RESULTS

Inhibition of Na^+/H^+ exchange in Caco-2 cell monolayers results in a rapid increase in TER. To determine whether Na^+/H^+ exchange affects transepithelial resistance in Caco-2 cells with active Na^+-glucose cotransport, we examined the effect of Na^+/H^+ exchange inhibitors on TER. Addition of 200 μM 5-(*N*,*N*-dimethyl)amiloride (DMA) resulted in a 36% ± 2% increase in TER ($P < 0.01$) within 30 min of DMA addition. Similar increases in TER were induced by other Na^+/H^+ exchange inhibitors (Fig. 1). We considered the possibility that increases in TER were due to cell swelling and collapse of lateral intercellular spaces. However, transmission electron microscopy of monolayers with increased TER due to incubation with up to 500 μM DMA showed that lateral intercellular space dimensions were indistinguishable from control cells. These data suggest that collapse of lateral intercellular spaces is not the explanation for the effect of Na^+/H^+ exchange inhibitors on TER.

Na^+/H^+ exchanger isoform specificity of TER increases. To determine if a particular Na^+/H^+ exchanger isoform was primarily responsible for the TER increases observed, we first characterized Na^+/H^+ exchanger isoform expression in the Caco-2 cell line studied. Previous studies have shown that Caco-2 cells, as well as most cell types, express NHE1. Although both NHE2 and NHE3 are present in the intestinal brush border (11), expression of these isoforms in Caco-2 monolayers varies between different Caco-2 clones (2, 5, 16). We evaluated NHE1, NHE2, and NHE3 expression in monolayers of the SGLT1-transfected Caco-2 cell clone used in this study. Expression of all three intestinal isoforms NHE1, NHE2, and NHE3 was detected (Fig. 2), although the NHE2 message detected was significantly less abundant than that for NHE1 and NHE3. Thus the Caco-2 clone used expressed NHE1, NHE2, and NHE3.

To determine which of these Na^+/H^+ exchanger isoforms was responsible for the effects of Na^+/H^+ exchange inhibitors on TER, we assessed the relative potency of amiloride and nonamiloride inhibitors of Na^+/H^+ exchangers. A rank potency of S-3226 > DMA > amiloride > clonidine > HOE-694 > cimetidine (Fig. 3) was determined. These data suggest that the apical Na^+/H^+ exchanger NHE3 is the critical target for the effect of these drugs on TER (Table 1). Further evidence in favor of NHE3 as the target is the insensitivity of TER to the Na^+/H^+ exchange inhibitor HOE-694, which inhibits NHE3 with an IC_{50} of 650 μM, but inhibits NHE1 and NHE2 with IC_{50} of 0.16 and 5 μM, respectively (4, 7).

To further define the role of NHE3 in TER regulation, we evaluated effects of the preferential NHE3 inhibitor S-3226. This agent inhibits NHE3 with an IC_{50} of 0.2–0.02 μM in porcine brush-border vesicles and human NHE3 expressed in fibroblasts but inhibits NHE1 and NHE2 isoforms at substantially greater IC_{50} of 3.5 and 80 μM, respectively (15). Because apical HCO_3^- transport has been reported to compensate for the absence of NHE3 in NHE3-deficient mice (12), these experiments were performed in nominally HCO_3^--free HBSS. Under these conditions, concentrations of S-3226 as low as 2 μM caused small, statistically significant increases in TER of 5 ± 1% ($P < 0.05$).

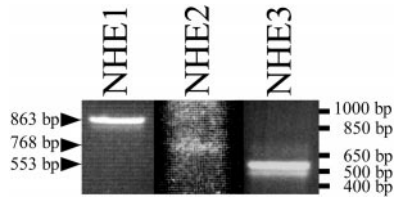

Fig. 2. Differentiated monolayers of Caco-2 cells express Na^+/H^+ exchangers 1, 2, and 3 (NHE1, NHE2, and NHE3). Agarose gel electrophoresis of PCR amplification reactions using primers specific for human NHE isoforms NHE1, NHE2, and NHE3. Single products were amplified for all primer pairs with expected sizes indicated by arrowheads (*left*; NHE1, 863 bp; NHE2, 768 bp; NHE3, 553 bp) and migration of size standards (*right*). Fivefold more reaction product from the NHE2 primer reaction was loaded to enhance detection. Control PCR reactions using intestinal cDNA (not shown) generated products that comigrated with those generated by amplification of Caco-2 cDNA.

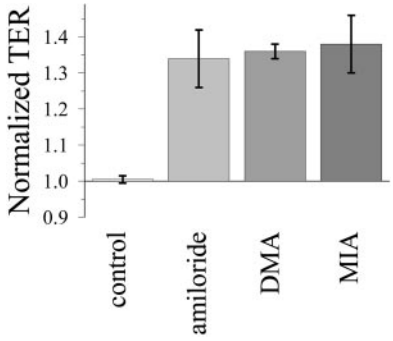

Fig. 1. Na^+/H^+ exchange inhibitors induce increases in transepithelial resistance (TER). Monolayers were incubated in Hanks' balanced salt solution (HBSS) for 30 min with 350 μM amiloride, 200 μM 5-(*N*,*N*-dimethyl)amiloride (DMA), or 50 μM 5-(*N*-methyl-*N*-isobutyl)amiloride (MIA) added to both sides of the monolayer. TER was measured and normalized to that of the control monolayers. TER of control monolayers was typically ~250 Ω·cm^2.

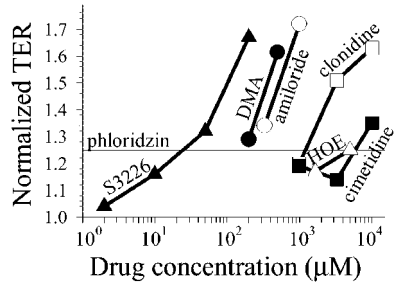

Fig. 3. Dose response and rank potency of Na^+/H^+ exchange inhibitor effect on TER. Monolayers were incubated with S-3226, DMA, amiloride, clonidine, HOE-694, or cimetidine. TER values were normalized to that of control monolayers. Drugs were added to both sides of each monolayer. The normalized TER 30 min after bilateral drug addition is shown. The horizontal line labeled "phloridzin" shows the physiological ~25% TER increases typically observed after inhibition of Na^+-glucose cotransport with phloridzin, a specific inhibitor of the Na^+-glucose cotransporter.

Table 1. *Rank potency of Na^+/H^+ exchange inhibitors in inducing increases in TER*

Effect	Rank Potency of Na^+/H^+ Exchange Inhibitors
TER increase	S-3226 > DMA > amiloride > clonidine > HOE-694 > cimetidine
NHE3 inhibition	S-3226 > DMA > amiloride > clonidine > HOE-694 > cimetidine
NHE1 inhibition	DMA > HOE-694 > amiloride > S-3226 > cimetidine > clonidine
NHE2 inhibition	DMA > amiloride > HOE-694 > cimetidine > clonidine > S-3226

The rank potency of Na^+/H^+ exchange inhibitors in inducing increases in TER was determined from the studies shown in Fig. 3. The rank potency of these inhibitors in inhibiting NHE1, NHE2, and NHE3 is taken from cited references (3, 4, 6, 15, 16). TER, transepithelial resistance; NHE, Na^+/H^+ exchanger; DMA, 5-(*N*,*N*-dimethyl)amiloride.

Addition of both 2 μM S-3226 and 50 μM HOE-694 (to inhibit NHE1 and NHE2) caused an increase in TER of 4 ± 1% ($P < 0.05$ vs. control with HOE-694 alone), which was not different from the effect of 2 μM S-3226 without HOE-694. Furthermore, by itself, 50 μM HOE-694 did not cause any increase in TER. Similarly, 10 μM S-3226 caused a 15 ± 4% increase in TER by itself ($P < 0.05$) and a 14 ± 3% increase in TER when combined with HOE-694 ($P < 0.05$). Thus when the effects of NHE1, NHE2, and apical HCO_3^- transport are eliminated, addition of the preferential NHE3 inhibitor S-3226 causes increases in TER that are quantitatively similar to increases in TER we have reported after inhibition of Na^+-glucose cotransport (22).

We also evaluated the ability of the preferential NHE3 inhibitor S-3226 to induce increases in TER when added only to apical or basal surfaces of the monolayer. Since NHE3 is only expressed apically, we anticipated that apical addition of S-3226 would cause the same degree of TER elevation as a bilateral drug addition but that basal drug addition would not. As shown in Fig. 4, apical S-3226 induced a 13 ± 1% increase in TER relative to monolayers not treated with S-3226 ($P < 0.005$). Similarly, bilateral S-3226 induced a 12 ± 1% increase in TER relative to monolayers not treated with S-3226 ($P < 0.015$). In contrast, basal S-3226 did not induce any increase in TER relative to monolayers not treated with S-3226 ($P > 0.4$). Thus despite the somewhat higher than expected doses of S-3226, as well as other Na^+/H^+ exchange inhibitors, needed to induce increases in TER, this effect seems to be mediated by apical Na^+/H^+ exchangers. Based on the published IC_{50} of S-3226 for basolateral NHE1, apical NHE2, and apical NHE3, these data are only consistent with an effect mediated by inhibition of NHE3.

Inhibition of Na^+/H^+ exchange leads to cytoplasmic acidification. We hypothesized that inhibition of Na^+/H^+ exchange might cause mild cytoplasmic acidification. Measurement of intracellular pH in BCECF-loaded cells showed that 20 μM DMA caused mild cytoplasmic acidification of 0.014 ± 0.001 pH unit ($P < 0.05$). This dose of DMA partially inhibited NHE3 (IC_{50} = 14 μM), completely inhibited NHE1 and NHE2 (IC_{50} of 0.1 and 0.7 μM, respectively), and had no effect on TER. These data suggest that although inhibition of NHE1 and NHE2 does cause a small decrease in intracellular pH (pH_i), this is insufficient to induce increases in TER. Similar small changes in pH_i without changes in TER were seen with 50 μM HOE-694. In contrast, 200 μM DMA caused pH_i to decrease by 0.026 ± 0.003 pH unit and also caused marked TER increases (see Fig. 6). Similar pH_i decreases and TER increases were also seen with other Na^+/H^+ exchange inhibitors at doses that inhibit NHE3. Thus these data suggest that inhibition of Na^+/H^+ exchange, particularly NHE3, results in both cytoplasmic acidification and increased TER in intestinal epithelial cells with ongoing Na^+-glucose cotransport.

NHE3 inhibition only causes TER increases when Na^+-glucose cotransport is active. The hypothesis that NHE3 is an intermediate in Na^+-glucose cotransport-dependent tight junction regulation predicts that NHE3 inhibition should only affect TER when Na^+-glucose cotransport is active. To test this prediction, the effect of S-3226 on TER was determined in the presence or absence of the specific Na^+-glucose cotransporter inhibitor phloridzin (Fig. 5). As shown, 10 or 25 μM S-3226 caused 7 ± 1% and 21 ± 1% increases in TER, respectively, in the presence of active Na^+-glucose cotransport (normalized to control monolayers with glucose, $P < 0.02$ for each S-3226 dose). When Na^+-glucose cotransport was inhibited with 2 mM phloridzin, TER increased by 28 ± 1% relative to monolayers with active Na^+-glucose cotransport ($P < 0.001$). Addition of 10 or 25 μM S-3226 in the presence of phloridzin did not cause significant increases in TER beyond the increases caused by phloridzin alone ($P > 0.1$ for each S-3326 dose vs. phloridzin without S-3226). Thus NHE3 inhibition only induces TER increases when Na^+-glucose cotransport is active.

Na^+/H^+ exchange inhibitors do not prevent Na^+-glucose cotransport. Since the effects of the Na^+/H^+ exchange inhibitors on both pH_i and TER overlapped with those observed after inhibition of Na^+-glucose cotransport with phloridzin (22), we considered the possibility that the Na^+/H^+ exchange inhibitors were blocking SGLT1-mediated Na^+-glucose cotransport.

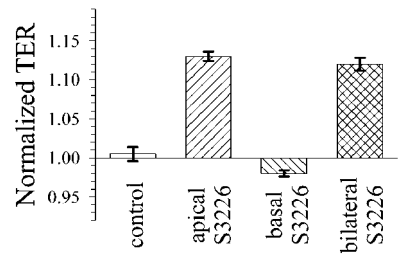

Fig. 4. S-3226 induces TER increases when added apically, but not when added basolaterally. Monolayers were incubated in HBSS (control), HBSS with 25 μM apical S-3226, HBSS with 25 μM basal S-3226, or HBSS with 25 μM S-3226 on both sides of the monolayer (bilateral). TER values after 30 min of drug exposure were normalized to that of the control monolayers.

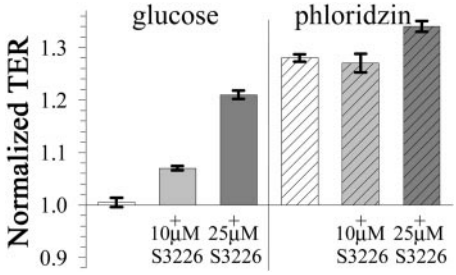

Fig. 5. Increased TER is only elicited by S-3226 when accompanied by active Na^+-glucose cotransport. One set of monolayers was incubated under standard conditions in HBSS with 25 mM glucose to allow active Na^+-glucose cotransport (glucose). A second set of monolayers was incubated in HBSS in which mannose was substituted for glucose, and 2 mM phloridzin, a specific Na^+-glucose cotransport inhibitor, was included to prevent active Na^+-glucose cotransport (phloridzin). S-3226 at 10 or 25 μM was added to monolayers in each group as indicated. TER values were normalized to that of the "glucose" monolayers (without S-3226). For this experiment, 60-min time points are shown to allow for the full effect of activating or inhibiting Na^+-glucose cotransport to become apparent. S-3226 data were similar at 30 min.

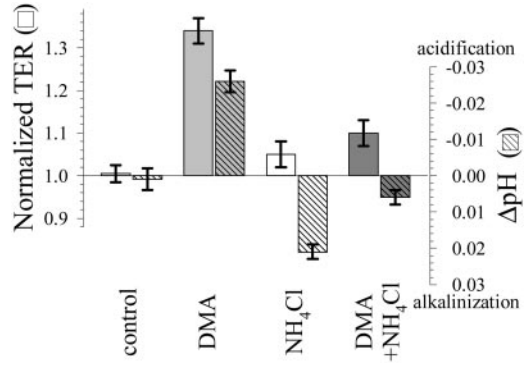

Fig. 6. NH_4Cl prevents TER increases and cytoplasmic pH decreases induced by Na^+/H^+ exchange inhibitors. Monolayers were incubated in HBSS, HBSS with 200 μM DMA, HBSS with 5 mM NH_4Cl, or 5 mM NH_4Cl combined with DMA. NH_4Cl and/or DMA was added to both apical and basal media. As shown on the left axis, TER values (open bars) after 30 min of drug exposure were normalized to that of the control monolayers (without NH_4Cl). Only the increased TER induced by DMA without NH_4Cl is statistically significant. Intracellular pH (pH_i; right axis, hatched bar) was determined in cells incubated under identical conditions. Changes in pH_i are shown with acidification (decrease in pH_i) moving upward along the *y*-axis and alkalinization (increase in pH_i) moving downward.

SGLT1 activity was measured using the nonmetabolizable glucose analog α-methyl-[^{14}C]glucoside, which cannot be transported by the facilitated glucose transporter GLUT-2 and, therefore, accumulates intracellularly (20). [^{14}C]methyl α-glucoside uptake in the presence of 200 μM DMA was 91 ± 8% of uptake in the absence of DMA. Thus inhibition of Na^+-glucose cotransport is not the mechanism by which the Na^+/H^+ exchange inhibitors elevate TER.

Cytoplasmic alkalinization prevents TER increases after inhibition of Na^+/H^+ exchange. In monolayers pretreated with 5 mM NH_4Cl, pH_i increased by 0.027 ± 0.003 pH unit ($P < 0.01$, Fig. 6). Subsequent addition of 200 μM DMA resulted in a decrement of pH_i by 0.021 ± 0.002 pH unit ($P < 0.01$), yielding a final pH_i that remained slightly more alkaline (0.006 ± 0.002 pH units) than that of control cells. Thus 5 mM NH_4Cl prevented the cytoplasmic acidification produced by 200 μM DMA. We used this observation to test whether the mild acidification caused by DMA was necessary for the TER increases. TER increases of 34 ± 5% were induced by 200 μM DMA ($P < 0.05$ compared with control). In contrast, when DMA was added to monolayers pretreated with 5 mM NH_4Cl, TER increases were reduced to 10 ± 5% (Fig. 6, $P < 0.05$ compared with DMA without NH_4Cl). Addition of NH_4Cl in the absence of Na^+/H^+ exchange inhibition did not significantly alter TER (Fig. 6). Thus cytoplasmic alkalinization by NH_4Cl prevents the effects of Na^+/H^+ exchanger inhibition on TER, suggesting that regulation of cytoplasmic pH may be part of the mechanism by which Na^+/H^+ exchange inhibitors effect increased TER.

Increased TER after inhibition of Na^+/H^+ exchange is accompanied by decreased MLC phosphorylation. Since we have previously shown that MLC phosphorylation is associated with Na^+-glucose cotransport-mediated regulation of TER (22), we hypothesized that this same pathway might be involved in the observed effects of NHE3 inhibition on TER. As assessed by ^{32}P incorporation into MLC in monolayers with active Na^+-glucose cotransport, addition of 1 mM amiloride or 200 μM DMA resulted in decreases in MLC phosphorylation of 28 ± 5% and 17 ± 6%, respectively (Fig. 7). Similarly, stoichiometric analysis of MLC phosphorylation showed a 43 ± 5% reduction in monophosphorylated MLC and a compensatory increase in nonphosphorylated MLC after incubation with 200 μM DMA (Fig. 8).

TER increases induced by MLC kinase inhibitors and Na^+/H^+ exchange inhibitors are not additive. Although the above data show that decreased MLC phosphorylation occurs following inhibition of Na^+/H^+ exchange, particularly NHE3, they do not directly address the role of MLC phosphorylation in TER regulation following NHE3 inhibition. To determine whether decreased phosphorylation of MLC was the

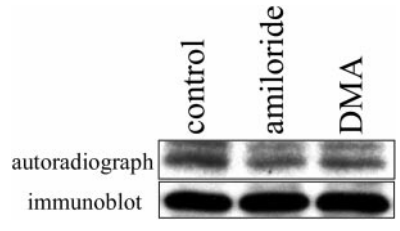

Fig. 7. ^{32}P incorporation into myosin light chain (MLC) is decreased by Na^+/H^+ exchange inhibitors. Monolayers were loaded with ^{32}P and incubated in phosphate-free HBSS (control) or phosphate-free HBSS with 1 mM amiloride or 200 μM DMA added to apical and basal media. ^{32}P incorporation was assessed by densitometry of the MLC band, as identified by anti-MLC autoradiography (*top*) and anti-MLC immunoblot (*bottom*) of 15% SDS-PAGE gels. The density of each MLC band on the autoradiograph was normalized to the corresponding band on the immunoblot to control for small variations in sample loading. Normalized ^{32}P incorporation into MLC decreased by 28 and 17% at 30 min after addition of 1 mM amiloride or 200 μM DMA, respectively.

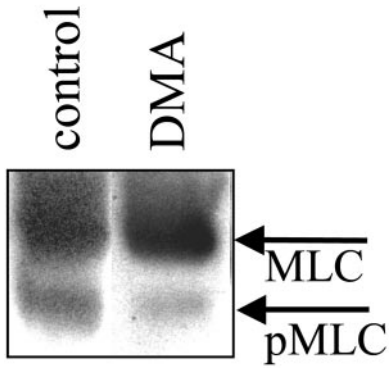

Fig. 8. MLC phosphorylation is decreased after addition of DMA. Monolayers were incubated in HBSS (control) or HBSS with 200 μM DMA. Cell lysates were separated on urea glycerol gels, and MLC isoforms were detected by immunoblot. A 43% reduction in monophosphorylated MLC (pMLC) was induced by treatment for 30 min with 200 μM DMA added to apical and basal media.

mechanism by which NHE3 inhibition increased TER, we evaluated whether inhibition of MLC kinase, which also decreased MLC phosphorylation, would be additive with the effects of NHE3 inhibition. The MLC kinase inhibitor ML-7 (20 μM) induced increases in TER of 48 ± 1% ($P < 0.01$). We showed this effect previously and also documented that ML-7 causes decreases in MLC phosphorylation that are similar to those that follow inhibition of Na^+-glucose cotransport (22). In this experiment, 200 μM DMA induced a 46 ± 4% increase in TER ($P < 0.01$). When DMA and ML-7 were applied together, the elevation in TER was 47 ± 6% (Fig. 9). Thus the effects of Na^+/H^+ exchange inhibitors and MLC kinase inhibition are not additive. This suggests that MLC kinase inhibition and Na^+/H^+ exchange inhibition may affect TER via a common distal signaling pathway.

DISCUSSION

We have previously shown that intestinal epithelial tight junction permeability is increased following activation of SGLT1-mediated Na^+-glucose cotransport (10, 22). This tight junction regulation occurs in vivo (13, 19), in isolated rodent small intestinal mucosa (1, 10), and in an intestinal epithelial cell culture model (20, 22). In the latter system, increased tight junction permeability is accompanied by phosphorylation of the myosin II regulatory light chain, and both MLC phosphorylation and tight junction regulation can be prevented by MLC kinase inhibitors (22). Thus it appears that increased MLC phosphorylation is a necessary intermediate in the intracellular signaling cascade that leads to increased tight junction permeability following activation of Na^+-glucose cotransport.

Transport of osmotically active solutes, such as Na^+ and glucose, leads to cell swelling. Such cell swelling triggers a regulatory volume decrease response (8) that, in isolated villus enterocytes, may require active Na^+/H^+ exchange (9). We hypothesized that mechanisms of regulatory volume decrease might overlap with those that mediate tight junction regulation. Thus we evaluated the role of Na^+/H^+ exchange in tight junction regulation. Inhibition of Na^+/H^+ exchange, particularly the apical intestinal Na^+/H^+ exchanger NHE3, caused decreased MLC phosphorylation and decreased tight junction permeability (increased TER). MLC phosphorylation and tight junction permeability also both decreased following termination of Na^+-glucose cotransport (22). Thus at least some events following inhibition of SGLT1-mediated Na^+-glucose cotransport or inhibition of NHE3-mediated Na^+/H^+ exchange are identical.

Although the data suggest that distal signaling events are shared between inhibition of SGLT1-mediated Na^+-glucose cotransport or inhibition of NHE3-mediated Na^+/H^+ exchange, a common proximal signaling pathway has not been demonstrated. However, the observation that NHE3 inhibition only caused increased TER in the presence of active Na^+-glucose cotransport suggests that Na^+-glucose cotransport and NHE3-mediated Na^+/H^+ exchange pathways for regulation of TER overlap. Moreover, if a common signaling pathway were involved, this model would predict that NHE3 is activated following initiation of SGLT1-mediated Na^+-glucose cotransport. In fact, we have recently observed NHE3-dependent cytoplasmic alkalinization following activation of Na^+-glucose cotransport (18). Thus NHE3 activation may indeed be an intermediate in the signaling pathway that links Na^+-glucose cotransport to tight junction regulation. Although incompletely defined, the role of NHE3 may be related to its effect on cytoplasmic pH. Thus it may be that Na^+-glucose cotransport leads to activation of NHE3, cytoplasmic alkalinization, increased MLC phosphorylation, perijunctional actomyosin ring contraction, and decreased TER. Inactivation of this hypothetical signaling pathway by inhibition of NHE3, as we have accomplished pharmacologically, would then lead to decreased tight junction permeability (increased TER).

Thus our studies show that inhibition of NHE3 results in increased TER. This effect requires the presence of active Na^+-glucose cotransport and also requires mild cytoplasmic acidification. Also, distal signaling events that mediate increases in TER, after either NHE3 inhibition or inhibition of Na^+-glucose

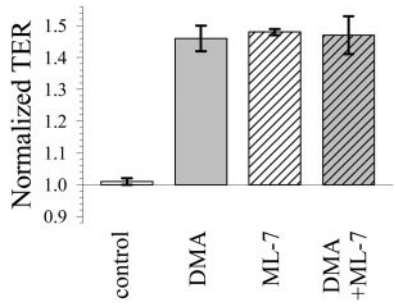

Fig. 9. TER increases induced by inhibition of Na^+/H^+ exchange or MLC kinase are not additive. Monolayers were incubated in HBSS (open bar) with 200 μM DMA, 20 μM ML-7, or DMA and ML-7. TER values were normalized to that of the control monolayers 30 min after addition of drugs to apical and basal media.

cotransport, overlap, since both are associated with decreased MLC phosphorylation. Thus we conclude that NHE3-dependent Na^+/H^+ exchange may be an intermediate in Na^+-glucose cotransport-dependent tight junction regulation.

We are grateful to Dr. H.-J. Lang for generously providing HOE-694 and S-3226. We also appreciate the assistance of Amy Ahearn and Yevegny Zolotarevsky.

This work was supported by National Institute of Diabetes and Digestive and Kidney Diseases Grants K08-DK-02503 (to J. R. Turner), R03-DK-56121 (to J. R. Turner), R37-DK-35932 (to J. L. Madara), R01-DK-26523 (to M. Donowitz), P01-DK-44484 (to M. Donowitz), and R01-DK-51116 (to C.-M. Tse).

REFERENCES

1. **Atisook K, Carlson S, and Madara JL.** Effects of phlorizin and sodium on glucose-elicited alterations of cell junctions in intestinal epithelia. *Am J Physiol Cell Physiol* 258: C77–C85, 1990.
2. **Bookstein C, Musch MW, Xie Y, Rao MC, and Chang EB.** Regulation of intestinal epithelial brush border Na^+/H^+ exchanger isoforms, NHE2 and NHE3, in c2bbe cells. *J Membr Biol* 171: 87–95, 1999.
3. **Brant SR, Yun CH, Donowitz M, and Tse CM.** Cloning, tissue distribution, and functional analysis of the human Na^+/H^+ exchanger isoform, NHE3. *Am J Physiol Cell Physiol* 269: C198–C206, 1995.
4. **Counillon L, Scholz W, Lang HJ, and Pouyssegur J.** Pharmacological characterization of stably transfected Na^+/H^+ antiporter isoforms using amiloride analogs and a new inhibitor exhibiting anti-ischemic properties. *Mol Pharmacol* 44: 1041–1045, 1993.
5. **Janecki AJ, Montrose MH, Tse CM, de Medina FS, Zweibaum A, and Donowitz M.** Development of an endogenous epithelial Na^+/H^+ exchanger (NHE3) in three clones of caco-2 cells. *Am J Physiol Gastrointest Liver Physiol* 277: G292–G305, 1999.
6. **Kapus A, Grinstein S, Wasan S, Kandasamy R, and Orlowski J.** Functional characterization of three isoforms of the Na^+/H^+ exchanger stably expressed in Chinese hamster ovary cells. ATP dependence, osmotic sensitivity, and role in cell proliferation. *J Biol Chem* 269: 23544–23552, 1994.
7. **Levine SA, Montrose MH, Tse CM, and Donowitz M.** Kinetics and regulation of three cloned mammalian Na^+/H^+ exchangers stably expressed in a fibroblast cell line. *J Biol Chem* 268: 25527–25535, 1993.
8. **MacLeod RJ and Hamilton JR.** Volume regulation initiated by Na^+-nutrient cotransport in isolated mammalian villus enterocytes. *Am J Physiol Gastrointest Liver Physiol* 260: G26–G33, 1991.
9. **MacLeod RJ and Hamilton JR.** Activation of Na^+/H^+ exchange is required for regulatory volume decrease after modest "physiological" volume increases in jejunal villus epithelial cells. *J Biol Chem* 271: 23138–23145, 1996.
10. **Madara JL and Pappenheimer JR.** Structural basis for physiological regulation of paracellular pathways in intestinal epithelia. *J Membr Biol* 100: 149–164, 1987.
11. **Maher MM, Gontarek JD, Bess RS, Donowitz M, and Yeo CJ.** The Na^+/H^+ exchange isoform NHE3 regulates basal canine ileal Na^+ absorption in vivo. *Gastroenterology* 112: 174–183, 1997.
12. **Nakamura S, Amlal H, Schultheis PJ, Galla JH, Shull GE, and Soleimani M.** HCO-3 reabsorption in renal collecting duct of NHE-3-deficient mouse: a compensatory response. *Am J Physiol Renal Physiol* 276: F914–F921, 1999.
13. **Pappenheimer JR and Reiss KZ.** Contribution of solvent drag through intercellular junctions to absorption of nutrients by the small intestine of the rat. *J Membr Biol* 100: 123–136, 1987.
14. **Persechini A, Kamm KE, and Stull JT.** Different phosphorylated forms of myosin in contracting tracheal smooth muscle. *J Biol Chem* 261: 6293–6299, 1986.
15. **Schwark JR, Jansen HW, Lang HJ, Krick W, Burckhardt G, and Hropot M.** S3226, a novel inhibitor of Na^+/H^+ exchanger subtype 3 in various cell types. *Pflügers Arch* 436: 797–800, 1998.
16. **Tse CM, Levine SA, Yun CH, Montrose MH, Little PJ, Pouyssegur J, and Donowitz M.** Cloning and expression of a rabbit cDNA encoding a serum-activated ethylisopropylamiloride-resistant epithelial Na^+/H^+ exchanger isoform (NHE-2). *J Biol Chem* 268: 11917–11924, 1993.
17. **Turner JR, Angle JM, Black ED, Joyal JL, Sacks DB, and Madara JL.** Protein kinase C-dependent regulation of transepithelial resistance: the roles of myosin light chain and myosin light chain kinase. *Am J Physiol Cell Physiol* 277: C554–C562, 1999.
18. **Turner JR and Black ED.** SGLT1-mediated Na^+-glucose cotransport activates NHE3 via a p38 MAPK-dependent pathway. *Gastroenterology* 118: A870, 2000.
19. **Turner JR, Cohen DE, Mrsny RJ, and Madara JL.** Noninvasive in vivo analysis of human small intestinal paracellular absorption: regulation by Na^+-glucose cotransport. *Dig Dis Sci*. In press.
20. **Turner JR, Lencer WI, Carlson S, and Madara JL.** Carboxy-terminal vesicular stomatitis virus G protein-tagged intestinal Na^+-dependent glucose cotransporter (SGLT1): maintenance of surface expression and global transport function with selective perturbation of transport kinetics and polarized expression. *J Biol Chem* 271: 7738–7744, 1996.
21. **Turner JR and Madara JL.** Physiological regulation of intestinal epithelial tight junctions as a consequence of Na^+-coupled nutrient transport. *Gastroenterology* 109: 1391–1396, 1995.
22. **Turner JR, Rill BK, Carlson SL, Carnes D, Kerner R, Mrsny RJ, and Madara JL.** Physiological regulation of epithelial tight junctions is associated with myosin light-chain phosphorylation. *Am J Physiol Cell Physiol* 273: C1378–C1385, 1997.